Optimal Horn Antenna Design to Excite High-Order Gaussian Beam Modes from TE_{0m} Smooth Circular Waveguide Modes

Carlos del Río Bocio, Ramón Gonzalo, *Student Member, IEEE*,
Mario Sorolla Ayza, and Manfred Thumm, *Senior Member, IEEE*

***Abstract*— The availability of medium-power gyrotron tubes (10–30 kW, CW) at millimeter-wave frequencies (30–100 GHz) allows applications such as advanced ceramic sintering, surface coating, radar, remote sensing, deep-space communications, etc. The concept of high-order Gaussian beam modes, which, under some conditions, can be assumed to be free-space modes, is applied to transport efficiently the power generated by a gyrotron for technological applications. A family of optimized nonlinear horn antennas is investigated in order to get the maximum coupling between the guided output mode of the gyrotron and the Gaussian beam modes. The numerical simulations show very favorable coupling with a conversion efficiency of about 99.8%.**

***Index Terms*—Circular waveguides, Gaussian beams, horn antennas.**

I. Introduction

A microwave beam radiated from a circular waveguide with strongly reduced diffraction (suppression of sidelobes) is desired for a wide range of applications. In order to get it, the technique used up to now was to look for the proper waveguide aperture illumination design by playing with waveguide mode relations. To create a good far-field radiation pattern like that of the fundamental Gaussian beam mode, a mixture of corrugated circular waveguide HE_{1m} modes is required. Furthermore, for some specific applications, a hollow cone Gaussian beam is desirable and it can be generated by an appropriate mixture of smooth circular waveguide TE_{0m} modes. In [1]–[3], the previous work done in relation with this topic is presented. In these papers, the authors give some good mode mixtures to obtain a far-field pattern with reduced sidelobes. As an example, Fig. 1 shows the calculated and measured far-field radiation pattern of the mixture: TE_{01} (85%) and TE_{02} (15%) modes with proper phase working at 70 GHz and 27.8-mm inner waveguide diameter. A good agreement between the calculations and the measurements can be observed.

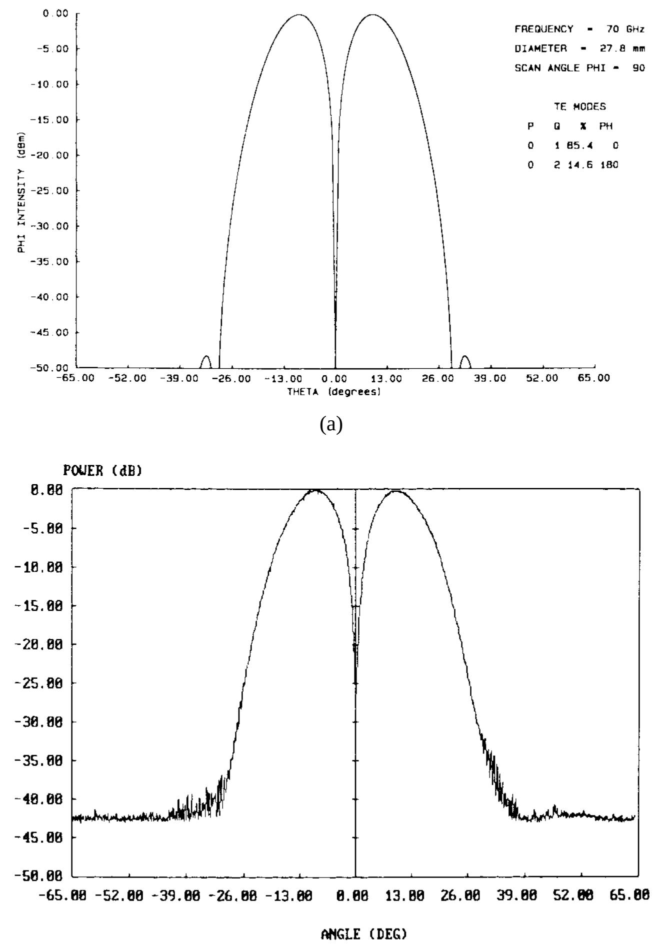

(a)

(b)

Fig. 1. Theoretical and experimental far-field intensity distribution of a properly phased TE_{01}/TE_{02} (85.4%/14.6%) mode mixture.

In this paper, we present a solution to achieve low sidelobe beams by means of an original and optimal nonlinear horn antenna to couple a waveguide field distribution to a free-space beam mode. Assuming paraxiality, we can consider some Gaussian beam mode families as functional basis of the beam solutions in this space [4], [5]. We will choose the family which fits as well as possible our geometrical restrictions imposed by the utilized waveguide. For instance, if we are working in a circular waveguide, the chosen basis would be the Laguerre–Gauss beam modes, and the optimal basis for

Manuscript received January 21, 1997; revised March 17, 1999. This work was supported by the Spanish (MEC) and German (BMBF) governments within the "Acciones Integradas Hispano Alemanas" over several years. The Spanish Team was supported by the CICYT under contract TIC95-0562-E.

C. Del Río Bocio, R. Gonzalo, and M. Sorolla Ayza are with the Microwave and Millimeter Wave Group, Universidad Pública de Navarra, Pamplona, Navarra, E-31006 Spain.

M. Thum is with Universität Karlsruhe, Institut für Höchstfrequenztechnik und Elektronik, Karlsruhe, D-76021 Germany, and with Forschungszentrum Karlsruhe, Institut für Technische Physik, Karlsruhe, D-76021 Germany.

Publisher Item Identifier S 0018-926X(99)07059-3.

the rectangular waveguide case would be the Hermite–Gauss beam-modes family [6], [7].

First, in order to validate the applied testing method, we will proceed to show the compatibility between these free-space Gaussian beam modes and the smooth waveguide modes, representing the far-field pattern of an open-ended waveguide as combination of Gaussian modes and conversely expanding the Gaussian beam modes as combinations of waveguide modes.

The profile of the proposed antenna is determined basically by the expansion formula of the Gaussian beam modes. From several "good field distributions" inside the waveguide (i.e., TE_{0m}, HE_{11} circular waveguide modes), we can excite very efficiently a pure Gaussian beam mode. In addition, we can consider these antennas as an optimal impedance matching device between the waveguide and the free-space.

In communication applications, the preferred mode to carry the power or information through the system is the fundamental Gaussian beam mode because of its low diffraction losses [8]. For material processing applications the final beam shape is not so relevant, because the experiment has to be done in an applicator having a metallic mode diffusor in order to obtain a uniform distribution of the electromagnetic field. Thus higher order Gaussian beam modes can be guided by an optimized high-order beam waveguide to the final applicator [9], [10]. The only problem in the design of a beam waveguide is how to generate the beam mode from the waveguide mode; this problem is solved by using the proposed horn antennas.

II. Gaussian Beam Modes and Waveguide Modes

In this paper, we will focus on the generation of high-order conical Gaussian modes from the smooth circular waveguide TE_{0m} modes. The waveguide modes are obtained directly as the output of a classical medium power gyrotron. Nevertheless, the principle presented here is also valid to generate the fundamental Gaussian beam mode from a corrugated circular waveguide HE_{11} mode and even for other cases with different waveguide geometries. In general, we can shape any oversized waveguide field distribution in order to obtain the Gaussian structure.

At this point, we study the compatibility of the selected basis inside and outside the antenna. For the inside basis, we can use the well-known waveguide modes because the horn antenna is a circular waveguide structure. To define the launched field outside the antenna, we can choose as the free-space beam mode the generating basis that is defined in [6]. For a coherent representation of a TE_{0m}-mode field distribution in terms of this basis we will need a large number of beam modes. By choosing a subfamily of these modes as generating basis, we are limiting the basis generation domain, but the number of eigenmodes necessary to represent TE_{0m} modes is considerably reduced.

Since the TE_{0m} modes are represented only by the azimuthal electric field component, the aim will be to look for circularly symmetric eigenmodes, which are defined only with the azimuthal component of the electric field like the TE_{0m} modes. Another important feature of the TE_{0m} modes is their zero on the propagation axis, thus, it will be very convenient if all the eigenmodes have also a zero on the propagation axis.

As a result of these considerations, we propose the following generating basis [10]:

$$\bar{\Psi}_m(r,\phi,z) = \Psi_m^{1,\frac{\pi}{2}}(r,\phi,z)\cdot\hat{x} + \Psi_m^{1,0}(r,\phi,z)\cdot\hat{y} \quad (1)$$

$\hat{x}$ and $\hat{y}$ are two orthogonal directions, and Ψ_m^{1,φ_0} are the Laguerre–Gaussian modes, which are solutions of the paraxial wave equation defined as [6]

$$\Psi_a^{b,\varphi_0}(r,\varphi,z) = \frac{1}{\sqrt{1+\xi^2}}\left(\frac{\sqrt{2}r}{\bar{\omega}_0\sqrt{1+\xi^2}}\right)^b \times\cos(b\varphi-\varphi_0)L_a^{(b)}\left(\frac{2r^2}{\bar{\omega}_0^2(1+\xi^2)}\right) \times e^{j(b+2a+1)tg^{-1}(\xi)}e^{-\frac{r^2}{\bar{\omega}_0^2(1-j\xi)}} \quad (2)$$

where, in the notation of cylindrical coordinates, r is the radius, φ the azimuthal angle, and $\xi = \lambda z/\pi\bar{\omega}_0^2$ is the normalized axial coordinate, $L_a^{(b)}$ are the generalized Laguerre polynomials, and $\bar{\omega}_0$ the beam waist defined as the minimum waist for the fundamental Gaussian mode, $\Psi_0^{0,0}$, in this case, located at $\xi = 0$. The fact that Ψ_a^{b,φ_0} is a solution of the scalar paraxial wave equation implies that each Cartesian component in (1) is a solution of Maxwell's equations.

If we combine two identical modes with $b = 1$, rotated around the axis by 90° to each other, as is proposed in (1), an azimuthally polarized concentric hollow cone distribution of the electric field is generated. The final expression for these modes of the new basis can be written as

$$\bar{\Psi}_m(r,\varphi,z) = \frac{1}{\sqrt{1+\xi^2}}\left(\frac{\sqrt{2}r}{\bar{\omega}_0\sqrt{1+\xi^2}}\right)L_m^{(1)}\left(\frac{2r^2}{\bar{\omega}_0^2(1+\xi^2)}\right) \times e^{j2(m+1)tg^{-1}(\xi)}\cdot e^{-\frac{r^2}{\bar{\omega}_0^2(1-j\xi)}}\cdot\hat{\varphi} \quad (3)$$

where the superindexes disappear as well as the azimuthal dependence. In Fig. 2, the power density in a plane perpendicular to the propagation axis of the first three modes is presented. From now on, we refer to these Gaussian modes as conical Gaussian modes, because of their shape in a transverse plane.

In order to test the compatibility between the inner waveguide basis, TE_{0m} modes and the above defined paraxial free-space basis Ψ_m, we will try, first of all, to represent the far-field radiation patterns of the TE_{0m} modes as a combination of free-space modes and then we will obtain the Gaussian far-field radiation pattern by combining TE_{0m} waveguide modes and radiating them from an open-ended circular waveguide.

A. Far-Field Pattern of TE_{0m} Modes as Combination of Conical Gaussian Beam Modes

To obtain the far-field pattern of the conical Gaussian beam modes is very simple because we know the analytical expressions of the electric fields everywhere. We simply have to look for the fields over a sphere of large radius

$$\mathrm{FFP}(\theta,\varphi) \propto \Psi_m(\rho\sin(\theta),\varphi,\rho\cos(\theta)) \quad (4)$$

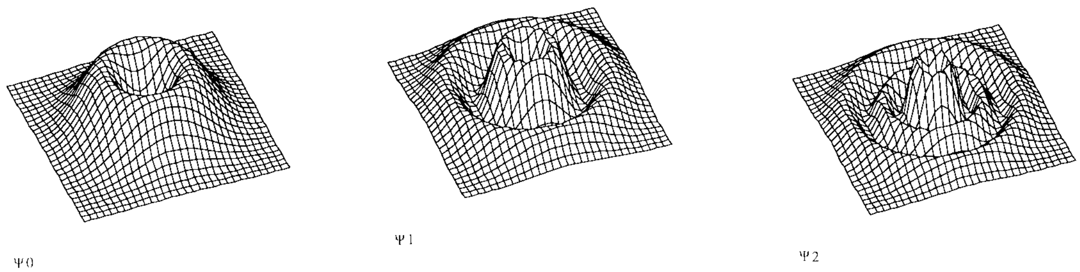

(a) (b) (c)

Fig. 2. Power density in a plane transverse to the propagation axis of the first three beam modes choosen as generating basis.

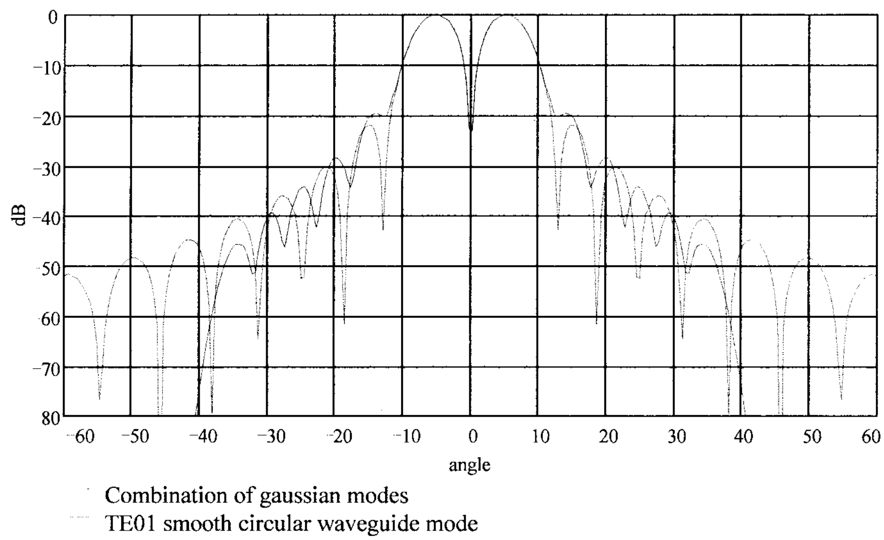

Fig. 3. Far-field radiation pattern of a TE_{01} waveguide mode and the linear combination of Gaussian beam modes to recover the TE_{01} waveguide mode (71.8% of Ψ_0, 25.5% of Ψ_1 and 1.9% of Ψ_2). ($f = 30.3$ GHz, $R = 50$ mm, $\bar{\omega}_0 = 20$ mm).

where ρ is the radius of the sphere. The azimuthal coordinate φ can be fixed because the far-field radiation pattern will be also symmetric, then we know the three-dimensional far-field radiation pattern with only one plane representation.

As it has been already shown, to fully define the electric field of the TE_{0m} waveguide modes and the conical Gaussian structures only the azimuthal component is necessary. Thus, we will reduce the problem to a two-dimensional one. Then we can decompose the azimuthal electric field component of the TE_{0m} waveguide modes in terms of the beam mode basis

$$E_{\varphi \mathrm{TE}_{0m}} = \sum_{n=0}^{\infty} C_{mn} \Psi_{\varphi n}, \qquad \text{for } m \geq 1 \tag{5}$$

where C_{mn} are the correlation coefficients calculated as

$$C_{mn} = \int_0^R E_{\varphi \mathrm{TE}_{0m}}(r, \varphi, z) \Psi_{\varphi n}(r, \varphi, z)^* \bigg|_{\varphi=0} 2\pi r \, dr \tag{6}$$

R being the waveguide radius where the TE_{0m} modes are defined.

For example, we will present the far-field pattern of a circular smooth waveguide TE_{01} mode radiated from an open-ended waveguide, using the conventional formalism [11] and [12], where the aperture effect has been neglected due to the oversized waveguide, and combining the corresponding conical Gaussian beam modes obtained with (5) and (6) (Fig. 3) to recover the TE_{01} waveguide mode. For the chosen conditions (working frequency of 30.3 GHz, inner waveguide radius of 50 mm and beam waist radius of 20 mm), the necessary mixture of Gaussian beam modes to represent the TE_{01} waveguide mode is

$$\Psi_0 \rightarrow 71.8\%, \quad \Psi_1 \rightarrow 25.5\%, \quad \Psi_2 \rightarrow 1.9\%, \quad \Psi_{n>2} \rightarrow 0.8\%.$$

The two curves of Fig. 3 are in very good agreement only for lower values of angle, clearly limited by the paraxial behavior of the conical Gaussian structures. If we change the working frequency, keeping constant the relation between the waveguide radius and the beam waist of the Gaussian structures, the needed conical Gaussian beam-mode mixture that represents the TE_{01} waveguide mode remains unchanged. Thus, in Fig. 4, the Gaussian beam-mode mixtures needed to represent the TE_{01} mode are plotted as a function of the ratio between the beam waist $\bar{\omega}_0$ and the waveguide radius R. A maximum coupling coefficient between the TE_{01} mode and the first conical Gaussian mode is found for $\bar{\omega}_0 = 0.565R$.

These results are independent of the frequency. Nevertheless, we will have to obey the paraxiality conditions for the Gaussian structures presented in [13] to consider these modes as free-space modes. This imposes a lower frequency limit to be accurate. Translating the paraxiality condition to these

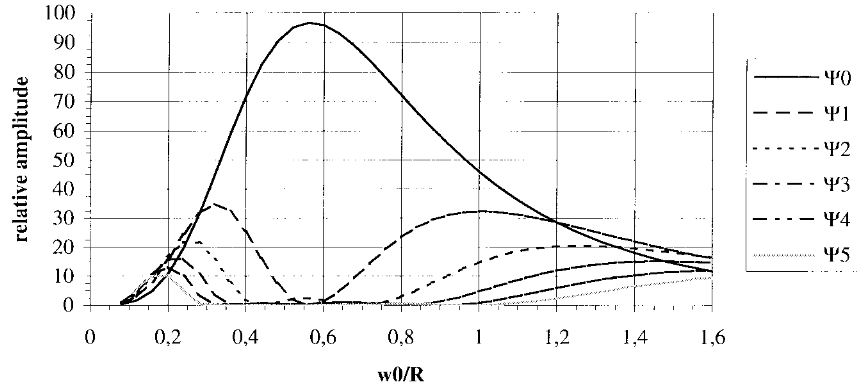

Fig. 4. Conical Gaussian beam mode ($\Psi_m; m = 0, \ldots, 5$) mixtures, representing the waveguide TE_{01} mode.

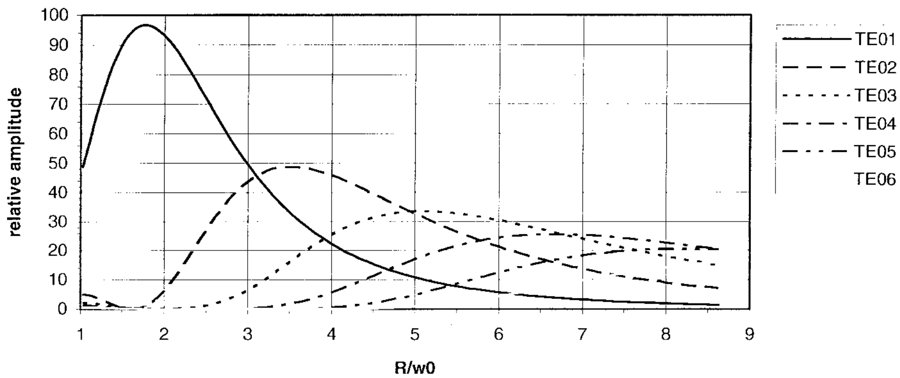

Fig. 5. TE_{0m} waveguide mode mixtures needed to represent a fundamental conical Gaussian mode Ψ_0.

conical modes, we obtain after some algebraic manipulations

$$k\bar{\omega}_0 > 6(m+2). \qquad (7)$$

where we have to remember that k is the free-space wavenumber, $\bar{\omega}_0$ the beam waist of the beam mode and m the radial index of the mode.

B. Representation of a Conical Gaussian Mode as Combination of TE_{0m} Modes

By means of an analogous procedure, we can obtain the TE_{0m} waveguide mode mixture necessary to represent a conical Gaussian beam mode. Now (5) has to be changed to the following:

$$\Psi_{\varphi n} = \sum_{m=1}^{\infty} C_{mn} E_{\varphi \mathrm{TE}_{0m}} \qquad (8)$$

where the C_{mn} are defined as in (6).

Now we can get some TE_{0m} mode combinations with a good Gaussian behavior, i.e., low sidelobe levels. In Fig. 5, the necessary TE_{0m} waveguide mode mixtures to get the conical Gaussian mode, Ψ_0, are plotted as a function of the ratio between the waveguide radius where the TE_{0m} modes are defined and the beam waist of the considered beam mode.

This figure has been calculated for $z = 0$ for which the coefficients are real numbers. Nevertheless, if we repeat the calculations for any value of z, the amplitude coefficients remain unchanged. But in order to represent correctly the natural diffraction effect of a Gaussian structure, a relative phase change is necessary.

As in the previous study, the curves represented in Fig. 5 are also independent of the operating frequency, and only the relation between the waveguide radius R and the beam waist $\bar{\omega}_0$ defines the desired mixture of TE_{0m} waveguide modes to achieve, as well as possible, a conical Gaussian beam field distribution.

III. Proposed Horn Antenna Profile

The selected profile should be appropriate to guide Gaussian structures and, simultaneously, it should have good matching properties at the interfaces to the waveguide and to the free-space. In order to fit as well as possible these desired features for the proposed antenna profile, we will expand the waveguide as the inner Gaussian structure expands, i.e.,

$$r(z) \propto \bar{\omega}_0 \sqrt{1 + \left(\frac{\lambda z}{\pi \bar{\omega}_0^2}\right)^2}. \qquad (9)$$

From the point of view of impedance matching, this profile can be a good solution, because it has a continuous derivative at the input, and a large radius at the output. Actually, Belousov *et al.* [14] proposed, as an optimal way to match the waveguide with the free-space, a very similar formula, which includes a higher order term, in order to take the field intensity smoothly off the wall of the horn.

To be consistent with the philosophy of the proposed antenna profile, the input waveguide field should have some

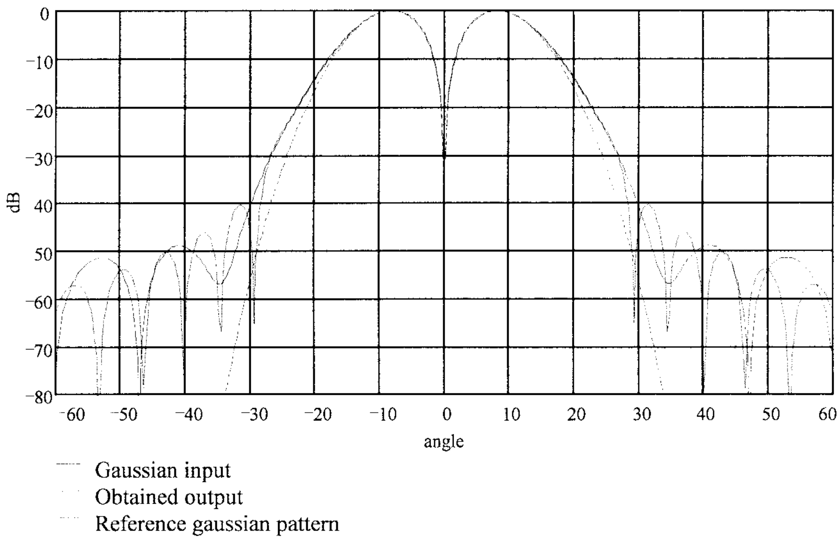

Fig. 6. Far-field radiation pattern of the Gaussian input and output of an antenna that are defined as combination of waveguide modes. The far-field pattern of the theoretical fundamental conical Gaussian mode is also presented.

Gaussian behavior. The similarity between the cross section of the TE_{01} and the Ψ_0 Gaussian field distributions is very high; for $\bar{\omega}_0 = 0.565R$, the cross correlation between both structures is about 96.7% (see Figs. 4 and 5). In relation to the phase, the beam waist of the antenna should be placed at the input; this means, constant phase along a plane at the input—the constant phase surfaces of the waveguide modes are assumed to be plane.

IV. Simulation Results

The first study should be to show the real possibility to guide Gaussian structures along the antenna, i.e., that the natural expansion in free-space of these Gaussian beam modes can be reproduced inside. In Fig. 6, we can see that the far-field pattern at the input and output of one antenna defined with (9) are in very good agreement. The input and the output are defined as TE_{0m} mode mixtures with about 99.95% of correlation factor with the real Gaussian structure. We only will have a window effect which generates some sidelobes in the far-field pattern. It is clear that the further away the waveguide structure is placed from the significant fields the more the window effect goes down. This means that we can use this profile to drive Gaussian structures, but nevertheless we would need at the input the same structure that we obtain as output.

In our case, the input will be the TE_{01} waveguide mode, which does not have a perfect Gaussian field distribution but has a high correlation factor. During the simulations, it has been observed that the initial TE_{01} mode distribution is gradually modified to a Gaussian structure at the end. This fact can be explained by means of the generation of a "transition area" at the input of the antenna. The presence of this transition area generates a small change of the beam waist in this part of the antenna. This can be understood as a change in the excited beam waist value and some shift in the position of the phase center, defined by the position of the beam waist.

In Fig. 7, the input beam waist value is represented as $\bar{\omega}_0$, and the obtained beam waist value $\bar{\omega}_0'$ shifted by Δz from the original phase center. However, the new asymptotic slope is in good agreement with the slope defined by the antenna due to the change of the beam waist value and the phase center shifting. Thus, in the final section of the antenna, a new Gaussian beam mode $\bar{\omega}'(z - \Delta z)$ is properly excited.

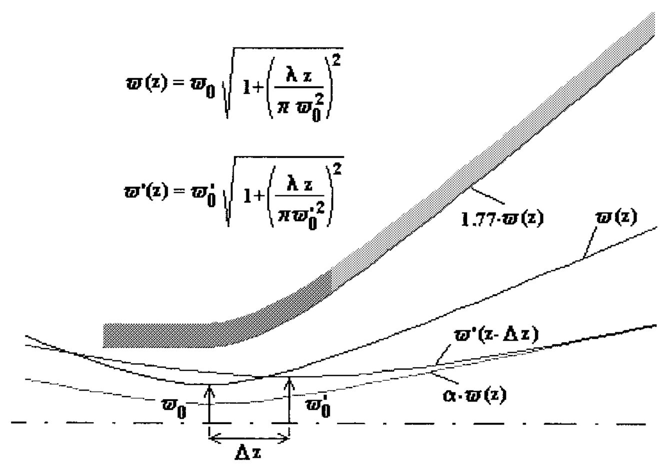

Fig. 7. Schematic representation of the effects on the beam waist and phase center.

Vlasov and Shapiro [15] propose a parabolic profile for such antennas to be used in a quasi-optical elbow. For some particular cases, the results obtained can be very similar with regard to the conversion efficiency. The reason why these two profiles, the Gaussian and the parabolic, are in some cases in good agreement is basically the similarity between the two curves during the "transition area" defined above (Fig. 8). And the most important problem for the parabolic profiles is that the area of coherent excitation of one particular Gaussian beam mode (in Fig. 7, shown for the case of a Gaussian profile, coincidence between the curves $\bar{\omega}'(z - \Delta z)$, excited Gaussian beam mode, and $\alpha\bar{\omega}(z)$, proportional to the antenna profile) is strongly reduced.

In Table I, the desired values for the ratio $\bar{\omega}_0/R$ used in the profile formula (9), and the obtained values for this

TABLE I
OBTAINED BEAM WAIST-INPUT RADIUS RATIO AND THE EFFICIENCIES VALUES FOR DIFFERENT ANTENNA LENGTHS

	$L=z_0$ $R_{out}=1.414R_{in}$		$L=1.5z_0$ $R_{out}=1.802R_{in}$		$L=2z_0$ $R_{out}=2.236R_{in}$		$L=2.5z_0$ $R_{out}=2.69R_{in}$		$L=3z_0$ $R_{out}=3.16R_{in}$	
ϖ_0/R_{in}	ϖ'_0/R_{in}	η (%)	ϖ'_0/R_{in}	η (%)	ϖ'_0/R_{in}	η (%)	ϖ'_0/R_{in}	η (%)	ϖ'_0/R_{in}	η (%)
0.55	0.6	99.723	0.61	99.84	0.61	99.826	-	-	-	-
0.54	0.595	99.736	0.605	99.87	0.61	99.877	-	-	-	-
0.53	0.595	99.74	0.605	99.897	0.605	99.91	-	-	-	-
0.52	0.595	99.728	0.6	99.916	0.605	99.925	0.605	99.921	0.605	99.913
0.51	0.59	99.7	0.6	99.92	0.6	99.934	0.6	99.928	0.605	99.924
0.50	0.59	99.67	0.595	99.918	0.595	99.927	0.6	99.924	0.6	99.926
0.49	0.59	99.6	0.595	99.9	0.595	99.9	-	-	0.595	99.91
0.48	-	-	0.59	99.87	0.59	99.874	-	-	-	-

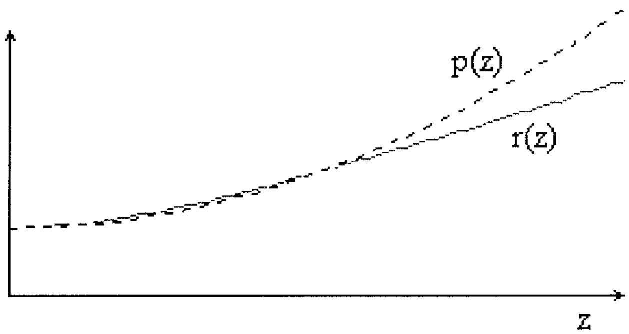

Fig. 8. Parabolic, $p(z)$, and Gaussian $r(z)$ profiles to excite the same Gaussian beam mode.

ratio, with the different conversion efficiencies, are presented. The conversion efficiency is defined as the correlation factor between the TE_{0m} output mode mixture and the excited conical Gaussian structure

$$\eta = \int_0^R \sum_m [E_{\varphi TE_{0m}}(r,\varphi,z)] \cdot \Psi_{\varphi 0}(r,\varphi,z{:}\bar{\omega}_0)^* \cdot 2\pi r\, dr \tag{10}$$

where R is the output radius. The parameter $\bar{\omega}_0$ and its position (related with the value of z) has to be optimized to get the maximum conversion efficiency to know which conical Gaussian beam has finally been excited.

Table I is calculated for the horn antenna lengths of z_0, $1.5z_0$, $2z_0$, $2.5z_0$, and $3z_0$, where $z_0 = \pi\bar{\omega}_0^2/\lambda$ is half of the Rayleigh distance. In all these cases, we will have practically the same results, theoretical efficiencies over 99.6%. It is important to remember that for different antenna lengths we will have different output radii and because of the beam waist value is approximately maintained, also different TE_{0m} output mode mixtures are needed (see Figs. 4 and 5).

Some important conclusions are obtained from these results. First of all, the presence of the transition area has been demostrated, because the input is the pure TE_{01} mode (correlation of 96.7%) and at the z_0 point the efficiency is higher than 99.6%, and the apparent beam waist value and its position have been modified. Due to the fact that the apparent beam waist value along the antenna is continuously increasing, the oversized factor of the significant fields inside the waveguide structure is also increasing, and then the efficiency can be a little bit higher. It is clear also that all the obtained ratios between waveguide radius and beam waist are close to the value 0.6. The input is always the TE_{01} waveguide mode, and this mode determines the equivalent input beam waist. By varying the coefficient used in the profile formula (9), $\bar{\omega}_0$, we can choose another output beam waist, losing some efficiency as a penalty.

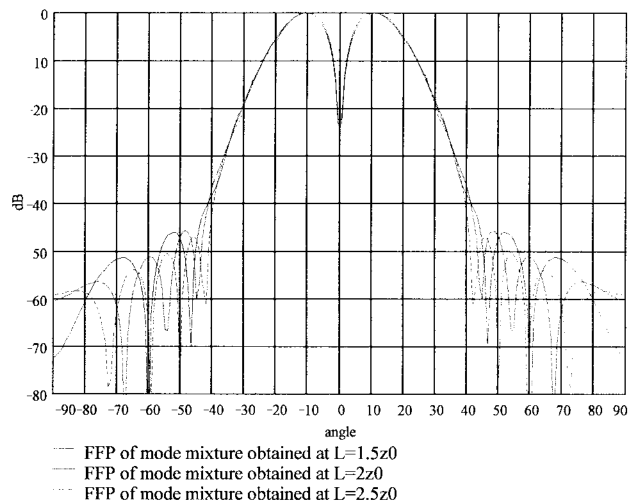

Fig. 9. Far-field radiation pattern of TE_{0m} waveguide mode mixtures presented in Table III.

By fixing the ratio $\bar{\omega}_0/R$ used in the profile formula (9) to 0.51 and cutting the antenna at different points $1.5z_0$, $2z_0$, and $2.5z_0$ the output radii will be $1.802R_{\rm in}$,$2.236R_{\rm in}$, and $2.69R_{\rm in}$, and, by knowing the output beam waist value (aproximate in all cases $0.6R_{\rm in}$), we could check the obtained TE_{0m} mode mixtures (Table II), which are in very good agreement with the abscissas 3.003, 3.726, and 4.483 of Fig. 5.

In Fig. 9, the far-field radiation patterns of the three TE_{0m} waveguide mode mixtures presented in Table II are shown. Despite of the different output radius values, the far-field pattern remains constant along the antenna. This is a proof that inside the antenna a Gaussian structure has been generated

TABLE II
RESULTS (POWER AND PHASE) FOR DIFFERENT LENGTHS OF THE ANTENNA DEFINED WITH $\bar{\omega}_0 = 0.51R_{\rm in}$, FED WITH A TE_{01} WAVEGUIDE MODE

	$L=1.5z_0$ $R_{out}=1.802R_{in}$		$L=2z_0$ $R_{out}=2.236R_{in}$		$L=2.5z_0$ $R_{out}=2.69R_{in}$	
Modes	%	**Phase**	%	**Phase**	%	**Phase**
TE_{01}	49.9483	83.527	28.5747	-144.52	15.865	-12.57
TE_{02}	43.2747	-49.92	48.2282	80.748	40.61	-152.1
TE_{03}	6.5951	-161	19.9385	-32.05	31.033	90.49
TE_{04}	0.1754	115.9	3.063	-123.6	10.44	-6.906
TE_{05}	----	----	0.18877	170.33	1.8382	-84.68
TE_{06}	----	----	----	----	0.193	-140.5

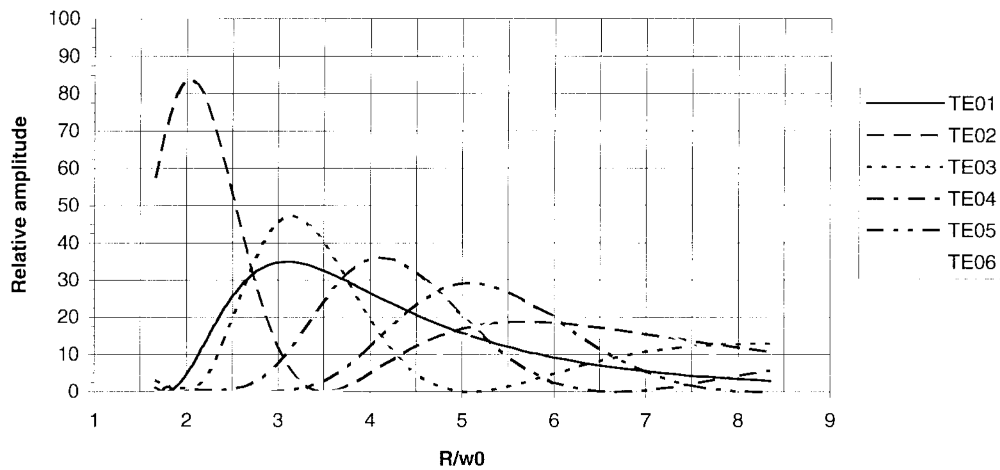

Fig. 10. TE_{0m} waveguide mode mixtures to represent a conical Gaussian beam mode Ψ_1.

and that it propagates toward the final part of the antenna. These antennas do not have an optimal length and we can cut the antenna anywhere over a minimum distance. In the case to feed the antenna with the TE_{01} mode, the minimum difference is approximately z_0.

In this paper, we have not given any working frequency. The results presented here are to some extent independent of the selected working frequency. Only in extreme cases we will have problems, i.e., frequencies and radius for which the needed mixture is impossible because some relevant modes are in cut-off. In others words, the paraxiality condition which defines the validity of the selected Gaussian beam modes must be satisfied.

V. GENERATING HIGHER ORDER MODES

For the first conical Gaussian beam mode, the design conditions have been presented. It is also possible to couple the second conical Gaussian beam mode Ψ_1 by exciting the antenna with a TE_{02} waveguide mode. The analogy between these two examples is clear and it can be easily generalized for higher order modes, $TE_{0m} \rightarrow \Psi_{m-1}$. It is easy to show that an efficient conversion will need a longer waveguide component as the input correlation factor is lower. The maximum correlation factor between the TE_{02} and the Ψ_1 modes is about 83.8% for $\bar{\omega}_0 = 0.49R$ (Fig. 10). For this case, the transition area is longer, the antennas should be longer as well, and the final obtained efficiencies are lower than the values of the previous case (96.6%).

Sweeping the beam waist values used in the profile formula (9), $\bar{\omega}_0 = 0.51R$ is found to be the optimum; this is the same as the value we used in the fundamental conical Gaussian mode case. We have a very interesting compatibility, the same antenna can be used to couple Ψ_0 from TE_{01} or Ψ_1 from TE_{02}. In the Table III, the obtained mixtures for different antenna lengths with $\bar{\omega}_0 = 0.51R$, are presented. The far-field pattern of these TE_{0m}-mode mixtures are plotted in Fig. 11. In this case, we can see that the coincidence between the curves is not as good as for the first conical Gaussian beam mode, but we have to remember that now the maximum efficiency is "only" 96.6%. The main problem to work with a higher conical Gaussian beam mode, is the diffraction, because it increases with the index of the mode. The angle needed to include at least 86% of the total carried power has to be increased for these conical Gaussian modes as follows:

$$\theta_m = \sqrt{2(m+1)}\theta_{0,0} \quad \theta_{0,0} = tg^{-1}(\pi\bar{\omega}_0/\lambda) \tag{11}$$

where $\theta_{0,0}$ is the needed angle for the fundamental Gaussian beam to include 86% of the total power.

In order to reduce the diffraction losses in the case of coupling higher order modes to free-space, one can introduce efficient rippled-wall mode transducers to convert the circular symmetric mode to a mode mixture appropriate for coupling to the first-order Ψ_0 mode [16]. This method has

TABLE III
RESULTS (POWER AND PHASE) FOR DIFFERENT LENGTHS OF THE ANTENNA DEFINED WITH $\bar{\omega}_0 = 0.51R_{\text{in}}$, FED WITH A TE_{02} WAVEGUIDE MODE

	$L=2z_0$ $R_{out}=2.236R_{in}$		$L=2.5z_0$ $R_{out}=2.69R_{in}$		$L=3z_0$ $R_{out}=3.16R_{in}$		$L=3.5z_0$ $R_{out}=3.64R_{in}$	
Modes	%	Phase	%	Phase	%	Phase	%	Phase
TE_{01}	29.088	-79.32	21.57	46.8	13.03	174.9	7.72	-52.4
TE_{02}	1.1405	-169.4	11.89	-70.38	20.6	46.7	20.35	167.3
TE_{03}	27.573	-140.3	7.363	-31.364	1.32	2.68	6.99	66.36
TE_{04}	30.5	134.98	30.5	-109.1	17.91	-2.479	5.37	89.77
TE_{05}	9.68	69.22	20.52	179.1	26.54	-75.7	22.52	25.52
TE_{06}	1.664	25.53	6.365	123.4	14.35	-138.6	21.6	-41.5
TE_{07}	0.302	1.382	1.38	85.015	4.61	172.1	10.56	-98.1
TE_{08}	----	----	0.3183	64.99	1.19	137.2	3.524	-142.5
TE_{09}	----	----	----	----	0.3	117.47	0.975	-174.9
TE_{010}	----	----	----	----	----	----	0.267	163.3

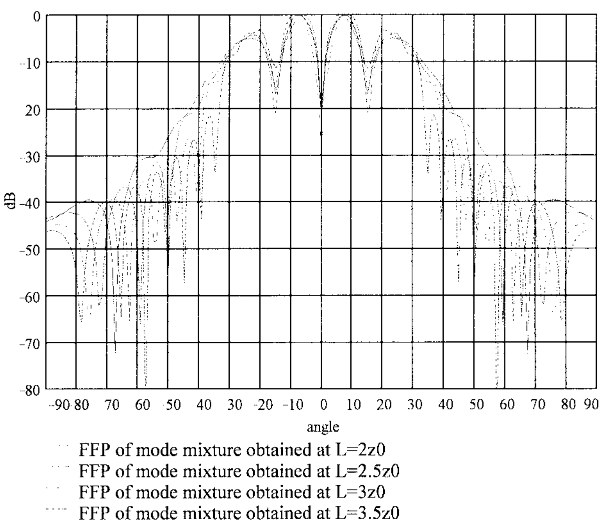

Fig. 11. Far-field radiation pattern of TE_{0m} waveguide mode mixtures presented in Table IV.

been very successfully verified in the transmission line of the compact technological gyrotron system at Forschungszentrum Karlsruhe where we achieved more than 90% transmission efficiency from the TE_{02} gyrotron to the applicator [9].

VI. CONCLUSION

An original and optimum antenna profile to couple waveguide modes to free-space modes (Gaussian beam modes) is presented. In particular, the coupling between the TE_{0m} waveguide modes and the conical Gaussian beam modes is considered. Once we have the Gaussian field distribution we can use quasi-optical techniques to propagate the power by multiple reflections at properly designed mirrors from the generator to the final cavity or experiment.

Depending on the application and the system restrictions, we can choose to generate a Ψ_0 or Ψ_1 conical Gaussian mode to carry the power through the quasi-optical transmission line, opening the possibility to build cheap and compact high-efficiency beam waveguides operating with high-order beam modes.

REFERENCES

[1] T. Graubner, K. Kasparek, and H. Kumric, “Synthesis and applications of special power distributions by HE_{1n} mode mixtures,” in *Int. Conf. Infrared Millemeter Waves Proc. Jpn. Soc. Antennas Propagat.*, Sendai, Japan, 1994, Cat. no. AP 941228, pp. 238–239.

[2] L. Rebuffi and M. Thumm, “Sidelobe suppression in radiated mode mixtures,” in *Int. Conf. Infrared Millimeter Waves Conf. Dig.*, Würzburg, Germany, 1989, pp. 154–155.

[3] L. Rebuffi, M. Thumm, and W. Henle, “A beam rectifier antenna system,” *Int. Conf. Infrared Millimeter Waves Conf. Dig.*, Würzburg, Germany, 1989, pp. 394–395.

[4] B. E. A. Saleh and M. C. Teich, *Fundamentals of Photonics*. New York: Wiley, 1991.

[5] M. Born and E. Wolf, *Principles of Optics*, 6th ed. New York: Pergamon, 1959, ch. 10.

[6] G. Wencker, “Rekursionsformeln und Entwicklungen der Strukturfunktionen Gaußscher Strahlen,” *A.U.E. Band 23*, pp. 521–523, 1969.

[7] D. H. Martin and J. W. Bowen, “Long wave optics,” *IEEE Trans. Microwave Theory Tech.*, vol. 41, pp. 1676–1690, Oct. 1993.

[8] P. F. Goldsmith, “Quasi-optical techniques at millimeter and submillimeter wavelengths,” *Int. J. Infrared Millimeter Waves*, vol. 6, ch. 5, pp. 277–343, 1982.

[9] A. Möbius, C. Del Río, M. Sorolla, and M. Thumm, “A hollow cone Gaussian beam quasioptical transmission line for a gyrotron technological system,” in *Int. Conf. Infrared Millimeter Waves, AT11 Conf. Proc.*, Berlin, Germany, July 1996.

[10] C. D. Río, M. Gonzalo, R. Sorolla, and M. Thumm, “Optimum horn antennas for high order mode beam waveguides,” in *Int. Conf. Infrared Millimeter Waves*, Orlando, FL, Dec. 1995, pp. 295–296.

[11] S. Silver, *Microwave Antenna Theory and Design.* Stevenage, U.K.: Peregrinus, 1984.

[12] P. Garin, L. Rebuffi, M. Thumm, and A. Jacobs, “Circular waveguide: Reference formulas for propagation and radiation,” *Int. Conf. Infrared Millimeter Waves*, Würzburg, Germany, 1989.

[13] C. del Río, R. Gonzalo, and M. Sorolla, “Paraxiality considerations of higher order Gaussian modes,” in *Int. Conf. Infrared Millimeter Waves, BTh6, Conf. Proc.*, Berlin, Germany, July 1996.

[14] V. I. Belousov, S. N. Vlasov, and L. V. Piskunova, “Izvestiya vysshikh uchebnikh zavedeniy,” *Seriya Radiofizika*, vol. 27, pp. 1214–1217, 1984.

[15] M. A. Shapiro and S. N. Vlasov, “Study of combined transmission line for high power wave generated by a gyrotron in the millimeter wavelength range,” *Int. J. Electron.*, vol. 72, nos. 5/6, pp. 1127–1133, 1992.

[16] C. D. Río, J. M. Net, J. Padulles, T. Sancho, M. Sorolla, M. Thumm, and A. Wien, “Undesired resonances in oversized rippled-wall mode converters,” *Int. J. Electron.*, vol. 77, no. 6, pp. 1101–1111, 1994.

Carlos del Río Bocio was born in Reus (Tarragona), Spain, on July 30, 1970. He received the Engineer degree in electronics from the Ramon Llull University, Barcelona, Spain, in 1993, and the Dr. Eng. degree from the Public University of Navarra, Spain, in 1996.

In 1991, he joined the Microwave Group in the Communications Department, Ramon Llull University, studying the resonant effects in rippled wall mode converters. Since 1993, he has been working with the Microwave Group of the Public University of Navarra, designing horns and quasi-optical transmission lines for high-order Gaussian beam modes. He was an Invited Scientist from 1996 to 1997 at the Gyrotron and Microwave Technology Department of the Forschungszentrum Karlsruhe, Germany. In March 1998 he became a Full Professor at the Public University of Navarra, where he teaches microwaves circuits and devices.

Ramón Gonzalo (S'95) was born on July 15, 1972 in Logroño, La Rioja, Spain. He received the M.S. degree in ingeniero de telecommunicación (with honors) from the Public University of Navarra (UPNa), Spain, in 1995. He is currently working toward the Ph.D. degree at European Space Research and Technology Center (ESTEC), Noordwijk, The Netherlands.

Since 1995, he has worked as Research Assistant to the Microwave Section in the Electrical and Electronic Department, UPNa. His current area of research is in the field of photonic band structures with emphasis on space antenna applications, design of waveguide transmission lines, and corrugated horn antennas.

Mr. Gonzalo he got a grant from the Spanish Government to work in ESTEC (ESA), in 1997.

Mario Sorolla Ayza was born in Vinaròs, Spain on October 19, 1958. He received the Telecommunication Engineering degree from the Politechnical University of Catalunya, Spain, in 1984, and the Doctor Engineer Degree in telecommunication from the Politechnical University of Madrid, Spain, in 1991.

From 1986 to 1990, he worked at the Association Euratom-Ciemat, Madrid, Spain, involved in the design of advanced high-power millimeter-wave transmission lines for plasma heating in magnetically confined fusion experiments. During this period he was Invited Scientist for 18 months at Institut für Plasmaforschung der Universität Stuttgart, Germany. There he worked in close cooperation with Dr. Thumm and his team on the design of waveguide components for the Spanish experiment TJ-II. He was Director of the Communications Department, Ramon Llull University, Barcelona, from 1991 to 1993 where he did research and teaching on microwaves, photonics, and antennas. He was in the private sector (Tagra and Mier) from 1984 to 1985 and from 1990 to 1991, respectively working in satellite communication microwave transceivers in microwave integrated circuits (MIC) and millimeter and microwave integrated circuits (MMIC) technologies. Since 1993 he has been a Full Professor at the Public University of Navarra, Pamplona, Spain, working with the Microwave and Millimeter Group and focused on high-power millimeter-wave components, numerical methods for their analysis and design, quasi-optical active circuits, and instruction on microwaves.

Dr. Ayza is a member of the IEEE Antennas and Propagation and Microwave Societies and ACES Society for Computational Electromagnetics.

Manfred Thumm (SM'94) was born in Magdeburg, Germany, on August 5, 1943. He received the Dipl. Phys. and Dr. rer. nat. degrees in physics from University of Tübingen, Germany, in 1972 and 1976, respectively.

At the University of Tübingen he was involved in the investigation of spin-dependent nuclear forces in inelastic neutron scattering. From 1972 to 1975, he was Doctoral Fellow of the Studienstiftung des deutschen Volkes. In 1976 he joined the Institute for Plasma Research, Electrical Engineering Department, University of Stuttgart, Germany, where he worked on RF production and RF heating of toroidal pinch plasmas for thermonuclear fusion research. From 1982 to 1990 his research activities were mainly devoted to electromagnetic theory in the areas of component development for the transmission of very-high-power millimeter waves through overmoded waveguides and of antenna structures for RF plasma heating with microwaves. In June 1990 he became a Full Professor at the Institute for Microwave and Electronics, University of Karlsruhe, Germany, and Head of the Gyrotron Development and Microwave Technology Division in the Institute for Technical Physics of the Research Center (Forschungszentrum), Karlsruhe. Since April 1999 he has been the Director of the Institute for Pulsed Power and Microwave Technology, Technical Physics of the Research Center (Forschungszentrum), where his current research projects are the development of high-power gyrotrons, windows, and transmission lines for nuclear fusion plasma heating and material processing.

Dr. Thumm is chairman of Chapter 8.6 (Vacuum Electronics and Displays) of the Information Technical Society (ITE) in the German VDE and a member of the German Physical Society (DPG).